THE JOURNAL OF PHYSICAL CHEMISTRY Letters

Letter

pubs.acs.org/JPCL

Charge Transfer or J-Coupling? Assignment of an Unexpected Red-Shifted Absorption Band in a Naphthalenediimide-Based Metal–Organic Framework

Brian D. McCarthy, Eric R. Hontz, Shane R. Yost, Troy Van Voorhis,* and Mircea Dincă*

Department of Chemistry, Massachusetts Institute of Technology, 77 Massachusetts Avenue, Cambridge, Massachusetts 02139-4307, United States

Supporting Information

ABSTRACT: We investigate and assign a previously reported unexpected transition in the metal–organic framework $Zn_2(NDC)_2(DPNI)$ (**1**; NDC = 2,6-naphthalenedicarboxylate, DPNI = dipyridyl-naphthalenediimide) that displays linear arrangements of naphthalenediimide ligands. Given the longitudinal transition dipole moment of the DPNI ligands, J-coupling seemed possible. Photophysical measurements revealed a broad, new transition in **1** between 400 and 500 nm. Comparison of the MOF absorption spectra with that of a charge transfer (CT) complex formed by manual grinding of DPNI and H_2NDC led to the assignment of the new band in **1** as arising from an interligand CT. Constrained density functional theory utilizing a custom long-range-corrected hybrid functional was employed to determine which ligands were involved in the CT transition. On the basis of relative oscillator strengths, the interligand CT was assigned as principally arising from π-stacked DPNI/NDC dimers rather than the alternative orthogonal pairs within the MOF.

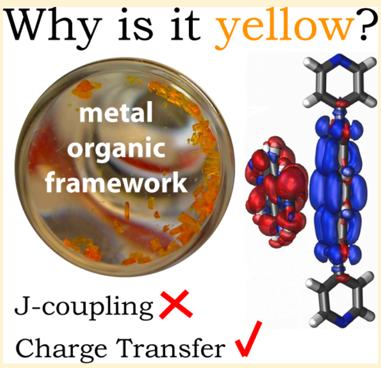

SECTION: Physical Processes in Nanomaterials and Nanostructures

The ability to define the packing of organic chromophores in molecular aggregates is paramount for understanding and controlling the photophysical processes in artificial light-harvesting constructs such as organic photovoltaics (OPVs). Inspiration toward this goal is often drawn from photosynthetic organisms, which efficiently trap photons and coherently transport excitons to a charge-separating center by using supramolecular architectures of light-absorbing chromophores such as chlorophylls and carotenes.[1−3] The challenge in mimicking the natural light-harvesting systems is to apply the photophysical and supramolecular organizational principles refined by nature in developing artificial materials that can harvest visible light and guide excitation energy transfer in a unidirectional manner. Many elegant synthetic solutions have been elaborated toward this goal. Dendrimers,[4−7] hyper-branched conjugated polymers,[8] and oligomeric porphyrin arrays,[9] for instance, show evidence of the electronic cooperativity necessary for efficient energy transfer. One particular architecture that has received attention to this end is that of J-aggregates. These are molecular constructs in which individual light-absorbing molecules are arranged such that their excitation dipole moments couple to promote delocalization of the excited state over many chromophores.[10] Whereas no single model for J-aggregate structure has been universally accepted, one widely acknowledged criterion is that such excitonic coupling occurs when the primary transition dipoles of the dye molecules are aligned head-to-tail.[10,11] J-aggregates are characterized by a red-shifted, narrow band with a high extinction coefficient that is frequently coupled to a fluorescence peak separated by only a very small Stokes shift. The interest in such aggregates from an OPV perspective stems from the advantages presented by this highly absorbing band: deliberate engineering of organic chromophores into J-aggregates could significantly reduce the required thickness of the light-absorbing layer, thereby reducing the likelihood of charge recombination losses. However, it is currently very difficult to control the solid-state packing of molecular chromophores, and J-aggregates historically have mostly been discovered by serendipity.

One class of materials that allows exquisite control over the intermolecular distances and angles between organic molecules is metal–organic frameworks (MOFs). These are crystalline hybrid materials made from inorganic and organic building blocks whose topologies, and implicitly the intermolecular distances between various building blocks, can be controlled by design using the principles of reticular chemistry. Although MOFs have traditionally been used for gas separation and storage, their highly ordered nature has also made them attractive targets for studying photophysical phenomena related to energy transfer[12−14] for light harvesting and luminescence for sensing.[15−17] The structure–function relationship of MOFs in relation to luminescence properties has also been the focus of recent careful studies.[15] Along the same lines, we envisioned

Received: December 13, 2012
Accepted: January 15, 2013

that the inherent ordered structure of MOFs could be conducive to J-aggregate formation in chromophores that do not normally exhibit this behavior if such chromophores could be aligned in the typical head-to-tail arrangement within MOFs. Furthermore, we surmised that given the extraordinary variety of MOF structures reported to date, J-coupling behavior may have gone unnoticed in some of the existing materials. We initially set out to investigate the possibility of J-coupling in the class of materials known as pillared MOFs. As shown in Figure 1, these are made from 2-D lattices containing one type of ligand and one type of secondary building unit and are connected in the third dimension by a second type of ligand — the pillar. Because the pillars are naturally aligned head-to-tail, we searched for materials in this class wherein the pillars were made of light-absorbing molecules. One promising candidate was quickly identified as $Zn_2(NDC)_2(DPNI)$ (**1**, NDC = 2,6-naphthalenedicarboxylate; DPNI = dipyridyl naphthalenediimide). Originally reported by Hupp et al., **1** was described as having an unexpected yellow color and weak luminescence despite the colorless nature of the individual building blocks: Zn^{2+} ions, NDC^{2-}, and DPNI.[18] Encouragingly, the supramolecular structure of **1**, shown in Figure 2a, reveals linear chains of DPNI pillars, a chromophore class well known to possess a primary transition dipole moment aligned with the long axis of the molecule.[19] Coupled to the reported unexpected yellow color and weak luminescence, it seemed feasible that J-coupling was occurring in **1**.

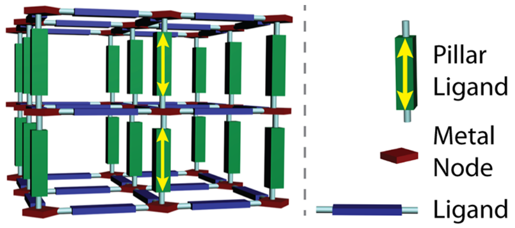

Figure 1. Schematic of a pillared MOF, with two types of organic ligands including the pillar. Yellow arrows indicate the transition dipoles and their expected head-to-tail arrangement within the chains defined by the pillar molecules.

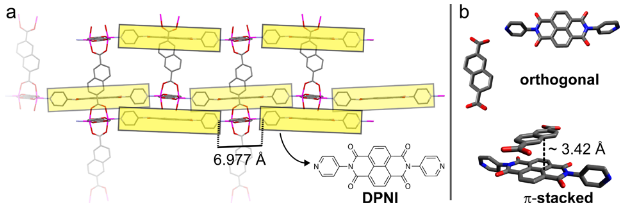

Figure 2. (a) Partial crystal structure of **1**. Outlined yellow boxes represent DPNI units. Faded yellow boxes indicate DPNI units located behind the first set due to framework interpenetration. (b) Two dimer pairs, orthogonal and π-stacked, of DPNI and NDC^{2-}. Gray, blue, red, and pink spheres represent C, N, O, and Zn atoms, respectively. Hydrogen atoms were omitted for clarity.

Although J-coupling in **1** seemed possible, it was clear that whereas numerous studies on MOFs exist, very few focus on explicitly interpreting bulk photophysical properties, and little established methodology is dedicated exclusively to interpreting the photophysical properties of MOFs. For instance, although many reports of photophysical properties of MOFs focus on fluorescence or luminescence, little effort has been devoted on understanding the influence of the supramolecular environment on the optical transitions. Additionally, whereas computational studies often help to elucidate the origins of photophysical properties in molecular species, little precedent exists for how such studies should be tuned for MOFs. Herein, we investigate the photophysical properties of **1** and present a theoretical framework for understanding its red-shifted absorption band, with a particular emphasis of modeling charge-transfer interactions in these intensively studied materials.

To facilitate the interpretation of the origin of the red-shifted band giving rise to the yellow color of **1**, a portion of its crystal structure is shown in Figure 2. Viewed along the *a* or *c* axes, linear chains of DPNI units, marked with yellow boxes in Figure 2a, are clearly visible. Each DPNI unit is separated from the next by 6.977 Å, which includes a $(Zn^{2+})_2$ cluster. Contrasting its arrangement with neighboring DPNI molecules, DPNI forms two distinct spatial relationships with NDC^{2-}. Within a single unit cell, DPNI is oriented orthogonal to the neighboring NDC^{2-} ligand with which it shares a $(Zn^{2+})_2$ cluster (Figure 2b). Two-fold interpenetration of **1** results in a second DPNI-NDC^{2-} interaction, in which the naphthalene core of a DPNI molecule in one framework π-stacks with a NDC^{2-} molecule of the second interpenetrated framework (Figure 2b).

Importantly, because the primary transition dipole of non core-substituted naphthalene diimides (NDIs) frequently lies directly along the long molecular axis,[20] and given the literature precedent for solution NDI J-aggregates,[21−24] it seemed feasible that J-coupling could occur along the chains of DPNI units observed in **1** and that such coupling is responsible for the red-shifted absorption band. Additionally, the DPNI−DPNI separation of 6.977 Å is within the range of interchromophore distances that are conducive of such coupling; for instance, reported J-aggregates of pyronine observed within channels of zeolite L are characterized by estimated interpyronine distances of 7.0 Å.[25] Furthermore, a calculation of the primary transition dipole of molecular DPNI confirmed that it lay directly along the long intermolecular axis (Table S2 in the Supporting Information), confirming the head-to-tail transition dipole arrangement that we hypothesized.

With J-coupling seemingly feasible by this structural analysis, compound **1** was synthesized and obtained as yellow needle-like crystals using a published procedure.[18] Diffuse reflectance UV−vis spectroscopy confirmed that **1** displays a new red-shifted broad transition between 400 and 500 nm, shown in Figure 3, which does not exist in the absorption spectra of the individual components DPNI and H_2NDC, also shown in Figure 3 (solid-state diffuse reflectance spectra of DPNI and H_2NDC are shown in Figure S3 in the Supporting Information). This contrasts with a recent investigation of **1**, which stated that the region above 400 nm was "featureless" despite the yellow nature of this compound.[26] The solution spectra of 2,6-H_2NDC and DPNI (Figure 3) show transitions located in the UV, with the prominent doublet peak of DPNI located between 350 and 400 nm, a peak representative of naphthalenediimides.[27] Notably, investigations of the reported weak visible range luminescence of pure samples of **1** using epifluorescence microscopy did not reveal any detectable signal. Further analysis using a conventional fluorimeter could not find detectable visible-region luminescence over a range of excitation wavelengths. However, impure batches of **1** (confirmed by extraneous powder X-ray diffraction peaks that are not predicted by a simulation of the PXRD pattern of **1**)

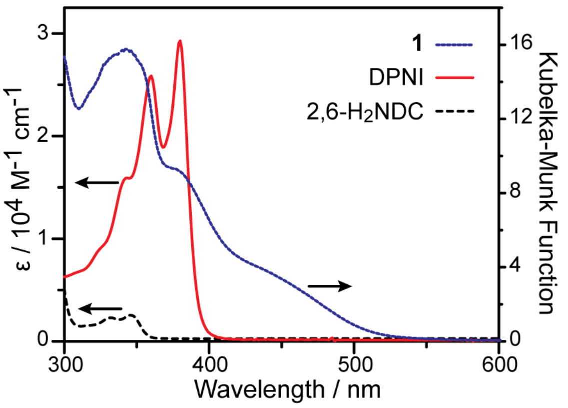

Figure 3. Solution molar absorptivities of DPNI and 2,6-H_2NDC in DMF and diffuse reflectance spectrum of **1**.

were luminescent under UV excitation, as shown in Figure S4b in the Supporting Information. Optical microscopy confirmed that small colorless crystals adhered to the yellow crystals of **1** in these impure samples (Figure S4a in the Supporting Information). Efforts to identify the colorless crystals from the additional PXRD peaks were unsuccessful. Altogether, these observations suggested that the originally reported weak fluorescence arose from a small amount of impurity in the crystal but that the red-shifted absorption band indeed originated from **1** itself. Importantly, the lack of fluorescence in **1**, which is atypical of J aggregation, was a first indication that this material may not in fact exhibit J-coupling. Furthermore, although J-aggregates with broad red-shifted features have been previously reported,[22,23,28,29] the broadness and relative weakness of the red-shifted band in **1** prompted us to evaluate alternative interpretations for the novel photophysical features in this material.

With J-coupling likely ruled out and the full d manifold of Zn^{2+} eliminating the possibility of d-d transitions, CT interactions were considered as a possible explanation instead. CT interactions could be envisioned to occur between any of the components of **1** (DPNI, NDC^{2-}, and/or the paddlewheel $Zn_2(O_2C-)_4$ cluster), or even across building blocks from the two interpenetrated frameworks. Ligand-to-metal or metal-to-ligand CT was deemed unlikely because it would result in a formal reduction or oxidation of the very stable d^{10} Zn^{2+} ion. Another possible CT interaction could occur between the framework and dimethylamine (DMA) formed by thermal decomposition of the DMF solvent during synthesis.[15c] Because the synthesis of **1** is carried out at a relatively low temperature (100 °C), little DMA is expected to have been formed. Recently, CT interactions between DPNI linkers and donor aromatic solvents were reported for a MOF similar to **1**.[15a,30] To simplify the CT analysis, the two organic components, DPNI and 2,6-H_2NDC, were considered first.

Motivated by a literature report of colored CT complexes formed by grinding DPNI and various small aromatics together in equimolar mixtures,[31] DPNI and 2,6-H_2NDC were ground together to yield solid-state complex **2** as a bright-yellow powder after several minutes. Convincingly, the diffuse reflectance UV−vis spectrum of **2**, shown in Figure 4a, displays a broad trailing transition between 400 and 500 nm that is similar in shape to the red-shifted absorption observed for **1**. PXRD analysis of **2** revealed several broad peaks, which were similar to peaks observed for isolated DPNI and 2,6-H_2NDC (Figure S5 in the Supporting Information). The presence of crystallinity in **2** is consistent with the formation of a DPNI/2,6-H_2NDC π-stacked material, as previously reported for DPNI CT complexes.[19] Importantly, the similarity between the red-shifted bands in **1** and **2** suggests that both can be attributed to CT interactions between 2,6-H_2NDC and DPNI. This assignment is indeed supported by a recent report of a different DPNI-containing MOF, which displays vastly shifted absorption profiles upon intercalation of various aromatics that act as donors.[32]

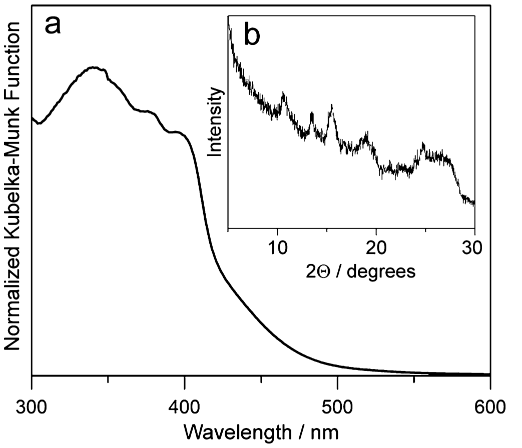

Figure 4. Diffuse reflectance spectrum and PXRD pattern (inset) of charge transfer complex **2**.

To investigate the assignment of the new band in **1** as a CT interaction instead of J-coupling, computational methods were utilized. The first excited singlet state of a DPNI monomer was found to have a considerable transition dipole moment of 13.6 D (with an oscillator strength of 0.49). However, the centers of mass of DPNI monomers within **1** are separated by ∼22 Å, which yields an estimated dipole−dipole coupling of only 2 meV. Because the spacing between the lowest energy electronic transition of DPNI and the middle of the broad band of **1** is about 450−500 meV, this estimated dipole−dipole coupling of 2 meV is too small to support assignment of the band as J-coupling.

With J coupling experimentally and theoretically ruled out, CT excitation energies were calculated for various dimer systems to support assignment of the new transition observed in **1** to an interligand CT. The π-stacked and orthogonal dimer systems shown in Figure 2b were considered. To account for the stabilization energy of the CT state due to the polarization of the surrounding molecules in the MOF, the dimer systems were embedded in a polarizable continuum with dielectric constant $\varepsilon = 2.0$ (a sample input file is included in the Supporting Information). The CT state energy was found to scale with ε, with larger ε values further stabilizing the CT state and lowering the excitation energy (Table S1 in the Supporting Information). The few reported dielectric constants for MOFs range from 4.6 to over 100,[33−35] but these simulations need to mimic the dielectric response at optical frequencies, which is typically much smaller. Thus, the dielectric constant was conservatively set to 2 but is possibly larger. Comparison of the oscillator strength for the π-stacked versus orthogonal dimer geometries suggested that CT happens predominantly within π-stacked dimers because the orthogonal geometry calculation yielded a very low oscillator strength (2.3×10^{-5}), whereas the π-stacked dimer gave a higher oscillator strength of 0.019.

Although basis set convergence for the CT energy of the simplified π-stacked system **2a** (Figure 5a) was reached with cc-PVTZ, the calculated energy range for the excitation (Table 1) remained higher than the experimentally observed band for **1**. To simulate the effect of the local charges on the CT energy, a model system dimer **2b** was built containing Zn^{2+} clusters on either end of the DPNI ligand truncated by acetate ions and ammonia molecules and is shown in Figure 5b. Indeed, the calculated energy for **2b** was lower than that of the dimer **2a**, but the use of the cc-PVTZ basis set was computationally prohibitive in this case. Consequently, the cc-PVTZ CT energy for **2b** was estimated from the difference in CT energy between the two basis sets for **2a**, ~0.1 eV, as shown in Table 1. This resulted in a CT excitation energy within the range observed experimentally for **1** and suggests that the presence of the positively charged Zn^{2+} ions facilitates stabilization of the accepted electron density on DPNI.

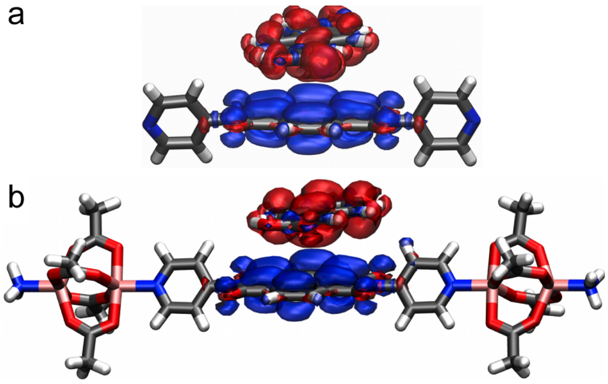

Figure 5. Two calculated charge-transfer states of dimers consisting of NDC^{2-} and DPNI (2a) and DPNI with capped $Zn_2(O_2CCH_3)_3$ linkage groups (2b). The electron and hole density changes are plotted as isosurfaces with the electron density in blue and the hole density in red.

Table 1. CT Excitation Energy Ranges of Dimer Systems (a) and (b) of Figure 5 Calculated Using CDFT with a Custom Long-Range-Corrected Functional

dimer system	basis set	CT energy (nm)[a]
(a)	6-31g*	337−378
(a)	cc-PVTZ	344−386
(b)	6-31g*	363−411
(b)	cc-PVTZ (estimated)	374−435

[a] Given 0.2 eV error bars.

Accordingly, the unexpected new red-shifted transition of **1** was assigned to an interligand DPNI/NDC^{2-} CT based on comparison with the CT complex **2**, an assignment that was supported computationally. Theoretical models also support the fact that the majority of the CT responsible for the new transition in **1** arises from π-stacked DPNI/NDC^{2-} units rather than orthogonal dimers. The lack of fluorescence from the MOF also lends credence to excitation of a CT state because nonradiative recombination of the CT states is often a very rapid process.[36] Although the more desirable J-coupling behavior was not observed in **1**, we have gained practical knowledge in what should be avoided in the design of MOFs with J-coupling and in how to accurately model these materials computationally. It is possible that the presence of the $(Zn^{2+})_2$ clusters directly between DPNI units interrupts coupling or, as our calculations suggest, that the inter-DPNI distance is too great for strong coupling. Interestingly, an analogous but noninterpenetrated MOF, $Zn_2(1,4\text{-NDC})_2(\text{DPNI})$, was reported to possess an orange color[37] despite the colorless nature of the ligands involved and a lack of π-stacking between 1,4-NDC^{2-} and DPNI. Efforts to cleanly duplicate the synthesis of this material and check the absorption spectrum for J-band or CT features were nevertheless unsuccessful. Additionally, a calcium MOF with NDI ligands was reported to have features in the visible region; these were attributed to intermolecular CT.[38]

The assignment of the new band in **1** to a CT interaction may have implications for prior reports of J-aggregation in NDIs that are also characterized by broad tailing bands rather than sharp transitions. Intriguingly, some of these reported NDI-based J-aggregates have side chains containing potential donating groups[23] that may participate in CT interactions. Efforts to design supramolecular J-aggregates in MOFs or other assemblies should be carried out with careful consideration of other potential interactions including CT, and this study underscores the importance of analyzing the extended structure for interpreting photophysical data. In the case of **1**, framework interpenetration resulted in well-aligned π-stacked donor/acceptor pairs. Whereas this structural motif did not lead to J-coupling, it could be used to facilitate energy transfer between π-stacked ligands in new MOFs. This report also highlights the utility of coupling synthetic design with computational studies, especially when targeting complex interchromophore interactions such as J-coupling in MOFs.

■ EXPERIMENTAL SECTION

Materials and Synthesis. 2,6-Naphthalenedicarboxylic acid (H_2NDC) (>98%, TCI America) and *N*,*N*-dimethylformamide (DMF, >99.8%, Macron Chemicals) were used as received. DPNI and $Zn_2(NDC)_2(DPNI)$ (**1**) were prepared as previously reported.[18] Purity was confirmed by ^1H NMR and by PXRD for DPNI and **1**, respectively (Figures S1 and S2 in the Supporting Information). Preparation of the DPNI/H_2NDC solid-state complex (**2**) was achieved by manually grinding an equimolar mixture of DPNI and H_2NDC for several minutes with an agate mortar and pestle.

Physical Measurements. A Varian Cary 5000 UV−vis-NIR spectrometer equipped with a Praying Mantis diffuse reflectance accessory (Harrick Scientific Products) was used to collect diffuse reflectance spectra, with $BaSO_4$ used as a white reference. Solution UV−vis spectra were obtained in DMF with an Agilent 8453 spectrometer. Extinction coefficients were determined by averaging the calculated molar absorptivity over five separate concentrations per compound. Epifluorescence micrographs and bright-field images were obtained using a Nikon Eclipse LV100 operating at ~380−400 nm excitation. NMR spectroscopy was performed with a 300 MHz Varian spectrometer. Powder X-ray diffraction (PXRD) patterns were obtained with a Bruker D8 Advance operating with $\theta/2\theta$ Bragg−Brentano geometry and using Ni-filtered Cu−Kα radiation (Kα1 = 1.5406 Å; 40 kV, 40 mA). Samples for PXRD were placed on a zero-background silicon crystal plate.

Computational Details. Typical functionals are known to yield inaccurate energies for CT excitation energies,[39,40] especially when using time-dependent density functional theory (TDDFT).[41] For this reason, a customized version of the

LC-ωPBE long-range-corrected[42] hybrid functional known to obtain accurate CT excitation energies[43] was used in all calculations. The range separation parameter ω and the amount of short-range Hartree−Fock exchange C_{HF} were tuned to match Koopman's theorem for the ionization potential of the neutral molecule and the anion[44−47] of DPNI. Further detail regarding this custom functional can be found in the Supporting Information. The transition dipole of the DPNI monomer unit was obtained from a TDDFT calculation using the 6-31G* basis set. The first 10 singlet excited states were calculated in all TDDFT calculations. The CT calculations were performed on dimer systems using constrained density function theory (CDFT)[48] by constraining an additional electron and spin on the acceptor molecule (the DPNI unit). For CT calculations, the dimers were embedded in a polarizable continuum[49] with a dielectric constant $\varepsilon = 2.0$ (this choice of dielectric constant is discussed in the main text of this manuscript). CDFT with configuration interaction (CDFT-CI)[50] between the ground and CT states was used to obtain the transition dipole for the CT excitation. All calculations were performed using the Q-Chem 3.1 computational package.[51]

■ ASSOCIATED CONTENT

Ⓢ Supporting Information

Powder X-ray patterns, epifluorescence micrographs, NMR spectra, additional computational results, details of computational methods, and sample Qchem input files. This material is available free of charge via the Internet at http://pubs.acs.org.

■ AUTHOR INFORMATION

Corresponding Author

*E-mail: mdinca@mit.edu (M.D.), tvan@mit.edu (T.V.V.).

Notes

The authors declare no competing financial interest.

■ ACKNOWLEDGMENTS

Research in the M.D. and T.V.V. groups was supported as part of the Center for Excitonics, an Energy Frontier Research Center funded by the U.S. Department of Energy, Office of Science, Office of Basic Energy Sciences under Award Number DE-SC0001088 (MIT). We thank Dr. Natalia Shustova for helpful discussions and Prof. Daniel Nocera for the use of a Praying Mantis accessory. Access to a Cary 5000 UV−vis-NIR was provided by the MIT Nanostructured Materials Metrology Lab sponsored by the Eni-MIT Solar Frontiers Center. NSF grants CHE-9808061 and DBI-9729592 provided support for the MIT NMR facility (DCIF). B.D.M. was supported by the MIT UROP program and the Amgen-UROP Scholars program.

■ REFERENCES

(1) Van Grondelle, R.; Dekker, J. P.; Gillbro, T.; Sundstrom, V. Energy Transfer and Trapping in Photosynthesis. *Biochim. Biophys. Acta* **1994**, *1187*, 1−65.

(2) Sener, M. K.; Olsen, J. D.; Hunter, C. N.; Schulten, K. Atomic-level Structural and Functional Model of a Bacterial Photosynthetic Membrane Vesicle. *Proc. Natl. Acad. Sci. U.S.A.* **2007**, *104*, 15723.

(3) Mcdermott, G.; Prince, S. M.; Freer, A. A.; Hawthornthwaite-Lawless, A. M.; Papiz, M. Z.; Cogdell, R. J.; Isaacs, N. W. Crystal-Structure of an Integral Membrane Light-Harvesting Complex from Photosynthetic Bacteria. *Nature* **1995**, *374*, 517.

(4) Jiang, D. L.; Aida, T. Photoisomerization in Dendrimers by Harvesting of Low-Energy Photons. *Nature* **1997**, *388*, 454.

(5) Mukhopadhyay, P.; Iwashita, Y.; Shirakawa, M.; Kawano, S.; Fujita, N.; Shinkai, S. Spontaneous Colorimetric Sensing of the Positional Isomers of Dihydroxynaphthalene in a 1D Organogel Matrix. *Angew. Chem., Int. Ed.* **2006**, *45*, 1592.

(6) Ceroni, P.; Bergamini, G.; Marchioni, F.; Balzani, V. Luminescence As a Tool to Investigate Dendrimer Properties. *Prog. Polym. Sci.* **2005**, *30*, 453.

(7) Bauer, R. E.; Grimsdale, A. C.; Mullen, K. Functionalised Polyphenylene Dendrimers and Their Applications. *Funct. Mol. Nanostruct.* **2005**, *245*, 253.

(8) Chen, L.; Honsho, Y.; Seki, S.; Jiang, D. Light-Harvesting Conjugated Microporous Polymers: Rapid and Highly Efficient Flow of Light Energy with a Porous Polyphenylene Framework as Antenna. *J. Am. Chem. Soc.* **2010**, *132*, 6742.

(9) Lin, V. S. Y.; Dimagno, S. G.; Therien, M. J. Highly Conjugated, Acetylenyl Bridged Porphyrins - New Models for Light-Harvesting Antenna Systems. *Science* **1994**, *264*, 1105.

(10) Würthner, F.; Kaiser, T. E.; Saha-Möller, C. R. J-Aggregates: From Serendipitous Discovery to Supra-molecular Engineering of Functional Dye Materials. *Angew. Chem., Int. Ed.* **2011**, *50*, 3376.

(11) Misawa, K.; Kobayashi, T. Hierarchical Structure in Oriented J-aggregates. In *J-Aggregates*; Kobayashi, T., Ed.; World Scientific Publishing: Singapore, 1996.

(12) Kent, C. A.; Liu, D.; Ma, L.; Papanikolas, J. M.; Meyer, T. J.; Lin, W. Light Harvesting in Microscale Metal-Organic Frameworks by Energy Migration and Interfacial Electron Transfer Quenching. *J. Am. Chem. Soc.* **2011**, *133*, 12940.

(13) Xie, Z.; Ma, L.; DeKrafft, K. E.; Jin, A.; Lin, W. Porous Phosphorescent Coordination Polymers for Oxygen Sensing. *J. Am. Chem. Soc.* **2010**, *132*, 922.

(14) Lee, C. Y.; Farha, O. K.; Hong, B. J.; Sarjeant, A. a; Nguyen, S. T.; Hupp, J. T. Light-Harvesting Metal-Organic Frameworks (MOFs): Efficient Strut-to-Strut Energy Transfer in Bodipy and Porphyrin-Based MOFs. *J. Am. Chem. Soc.* **2011**, *133*, 15858.

(15) (a) Takashima, Y.; Martínez, V. M.; Furukawa, S.; Kondo, M.; Shimomura, S.; Uehara, H.; Nakahama, M.; Sugimoto, K.; Kitagawa, S. Molecular Decoding Using Luminescence from an Entangled Porous Framework. *Nat. Commun* **2011**, *2*, 168. (b) Perry, J. J., IV; Feng, P. L.; Meek, S. T.; Leong, K.; Doty, F. P.; Allendorf, M. D. Connecting Structure with Function in Metal-Organic Frameworks to Design Novel Photo- And Radioluminescent Materials. *J. Mater. Chem.* **2012**, *22*, 10235. (c) Feng, P. L.; Leong, K.; Allendorf, M. D. Charge-Transfer Interactions in Luminescent Mofs: Implications for Solid-State Temperature and Environmental Sensing. *Dalton Trans.* **2012**, *41*, 8869.

(16) Shustova, N. B.; McCarthy, B. D.; Dincă, M. Turn-On Fluorescence in Tetraphenylethylene-Based Metal-Organic Frameworks: An Alternative to Aggregation-Induced Emission. *J. Am. Chem. Soc.* **2011**, *133*, 20126.

(17) Wanderley, M. M.; Wang, C.; Wu, C.-D.; Lin, W. A Chiral Porous Metal−Organic Framework for Highly Sensitive and Enantioselective Fluorescence Sensing of Amino Alcohols. *J. Am. Chem. Soc.* **2012**, *134*, 9050.

(18) Ma, B.-Q.; Mulfort, K. L.; Hupp, J. T. Microporous Pillared Paddle-Wheel Frameworks Based on Mixed-Ligand Coordination of Zinc Ions. *Inorg. Chem.* **2005**, *44*, 4912.

(19) Würthner, F.; Ahmed, S.; Thalacker, C.; Debaerdemaeker, T. Core-Substituted Naphthalene Bisimides: New Fluorophors with Tunable Emission Wavelength for FRET Studies. *Chem.—Eur. J.* **2002**, *8*, 4742.

(20) Bhosale, S. V; Jani, C. H.; Langford, S. J. Chemistry of Naphthalene Diimides. *Chem. Soc. Rev.* **2008**, *37*, 331.

(21) Avinash, M. B.; Govindaraju, T. Engineering Molecular Organization of Naphthalenediimides: Large Nanosheets with Metallic Conductivity and Attoliter Containers. *Adv. Func. Mater.* **2011**, *21*, 3875.

(22) Kumar, M.; George, S. J. Spectroscopic Probing of the Dynamic Self-Assembly of an Amphiphilic Naphthalene Diimide Exhibiting Reversible Vapochromism. *Chem.—Eur. J.* **2011**, *17*, 11102.

(23) Molla, M. R.; Ghosh, S. Structural Variations on Self-Assembly and Macroscopic Properties of 1,4,5,8-Naphthalene-diimide Chromophores. *Chem. Mater.* **2011**, *23*, 95.

(24) Shao, H.; Parquette, J. R. Self-Assembly of 1-D n-Type Nanostructures Based on Naphthalene Diimide-Appended Dipeptides. *Chem. Commun.* **2012**, *46*, 4285.

(25) Busby, M.; Blum, C.; Tibben, M.; Fibikar, S.; Calzaferri, G.; Subramaniam, V.; De Cola, L. Time, Space, and Spectrally Resolved Studies on J-Aggregate Interactions in Zeolite L Nanochannels. *J. Am. Chem. Soc.* **2008**, *130*, 10970.

(26) Usov, P. M.; Fabian, C.; D'Alessandro, D. M. Rapid Determination of the Optical and Redox Properties of a Metal—Organic Framework via in Situ Solid State Spectroelectrochemistry. *Chem. Commun.* **2012**, *48*, 3945.

(27) Pan, M.; Lin, X.-M.; Li, G.-B.; Su, C.-Y. Progress in the Study of Metal—organic Materials Applying Naphthalene Diimide (NDI) Ligands. *Coord. Chem. Rev.* **2011**, *255*, 1921.

(28) Shao, H.; Nguyen, T.; Romano, N. C.; Modarelli, D. a; Parquette, J. R. Self-Assembly of 1-D n-Type Nanostructures Based on Naphthalene Diimide-Appended Dipeptides. *J. Am. Chem. Soc.* **2009**, *131*, 16374.

(29) Busby, M.; Devaux, A.; Blum, C.; Subramaniam, V.; Calzaferri, G.; De Cola, L. Interactions of Perylene Bisimide in the One-Dimensional Channels of Zeolite L. *J. Phys. Chem. C* **2011**, *115*, 5974.

(30) Martínez-Martínez, V.; Furukawa, S.; Takashima, Y.; López Arbeloa, I.; Kitagawa, S. Charge Transfer and Exciplex Emissions from a Naphthalenediimide-Entangled Coordination Framework Accommodating Various Aromatic Guests. *J. Phys. Chem. C* **2012**, *116*, 26084.

(31) Trivedi, D. R.; Fujiki, Y.; Goto, Y.; Fujita, N.; Shinkai, S.; Sada, K. A Naked-Eye Colorimetric Indicator to Discriminate Aromatic Compounds by Solid-State Charge-Transfer Complexation. *Chem. Lett.* **2008**, *37*, 550.

(32) Takashima, Y.; Furukawa, S.; Kitagawa, S. Control of the Charge-Transfer Interaction between a Flexible Porous Coordination Host and Aromatic Guests by Framework Isomerism. *CrystEngComm* **2011**, *13*, 3360.

(33) Fu, D.-W.; Ge, J.-Z.; Dai, J.; Ye, H.-Y.; Qu, Z.-R. Synthesis, Structure and Dielectric Constant Properties of a Novel 1D Coordination Polymer$[K(2\text{-}PTA)(H_2O)]_n$. *Inorg. Chem. Commun.* **2009**, *12*, 994.

(34) Ye, Q.; Song, Y.-M.; Wang, G.-X.; Chen, K.; Fu, D.-W.; Chan, P. W. H.; Zhu, J.-S.; Huang, S. D.; Xiong, R.-G. Ferroelectric Metal—Organic Framework with a High Dielectric Constant. *J. Am. Chem. Soc.* **2006**, *128*, 6554.

(35) Fu, D.-W.; Ye, H.-Y.; Ye, Q.; Pan, K.-J.; Xiong, R.-G. Ferroelectric Metal-Organic Coordination Polymer with a High Dielectric Constant. *Dalton Trans.* **2008**, 874.

(36) Lakowicz, J. R. *Principles of Fluorescence Spectroscopy*; Springer: New York, 2006.

(37) Furukawa, S.; Hirai, K.; Takashima, Y.; Nakagawa, K.; Kondo, M.; Tsuruoka, T.; Sakata, O.; Kitagawa, S. A Block PCP Crystal: Anisotropic Hybridization of Porous Coordination Polymers by Face-Selective Epitaxial Growth. *Chem. Commun.* **2009**, 5097.

(38) Han, L.; Qin, L.; Xu, L.; Zhou, Y.; Sun, J.; Zou, X. a Novel Photochromic Calcium-Based Metal-Organic Framework Derived from a Naphthalene Diimide Chromophore. *Chem. Commun.* **2012**, *704*, 406.

(39) Autschbach, J. Charge-Transfer Excitations and Time-Dependent Density Functional Theory: Problems and Some Proposed Solutions. *ChemPhysChem* **2009**, *10*, 1757.

(40) Tawada, Y.; Tsuneda, T.; Yanagisawa, S.; Yanai, T.; Hirao, K. a Long-Range-Corrected Time-Dependent Density Functional Theory. *J. Chem. Phys.* **2004**, *120*, 8425.

(41) Runge, E.; Gross, E. K. E. Density-Functional Theory for Time-Dependent Systems. *Phys. Rev. Lett.* **1984**, *52*, 997.

(42) Iikura, H.; Tsuneda, T.; Yanai, T.; Hirao, K. A Long-Range Correction Scheme for Generalized-Gradient-Approximation Exchange Functionals. *J. Chem. Phys.* **2001**, *115*, 3540.

(43) Rohrdanz, M. A.; Martins, K. M.; Herbert, J. M. a Long-Range-Corrected Density Functional That Performs Well for Both Ground-State Properties and Time-Dependent Density Functional Theory Excitation Energies, Including Charge-Transfer Excited States. *J. Chem. Phys.* **2009**, *130*, 054112.

(44) Livshits, E.; Baer, R. a Well-Tempered Density Functional Theory of Electrons in Molecules. *Phys. Chem. Chem. Phys.* **2007**, *9*, 2932.

(45) Refaely-Abramson, S.; Baer, R.; Kronik, L. Fundamental and Excitation Gaps in Molecules of Relevance for Organic Photovoltaics from an Optimally Tuned Range-Separated Hybrid Functional. *Phys. Rev. B* **2011**, *84*, 075144.

(46) Baer, R.; Neuhauser, D. Density Functional Theory with Correct Long-Range Asymptotic Behavior. *Phys. Rev. Lett.* **2005**, *94*, 043002.

(47) Baer, R.; Livshits, E.; Neuhauser, D. Avoiding Self-Repulsion in Density Functional Description of Biased Molecular Junctions. *Chem. Phys.* **2006**, *329*, 266.

(48) Wu, Q.; Van Voorhis, T. Direct Optimization Method to Study Constrained Systems within Density-Functional theory. *Phys. Rev. A* **2005**, *72*, 024502.

(49) Tomasi, J.; Persico, M. Molecular Interactions in Solution: An Overview of Methods Based on Continuous Distributions of the Solvent. *Chem. Rev.* **1994**, *94*, 2027.

(50) Wu, Q.; Cheng, C.-L.; Van Voorhis, T. Configuration Interaction Based on Constrained Density Functional Theory: A Multireference Method. *J. Chem. Phys.* **2007**, *127*, 164119.

(51) Kong, J.; White, C. A.; Krylov, A. I.; Adamson, R. D.; Furlani, T. R.; Lee, S.; Lee, A. M.; Gwaltney, S. R.; Adams, T. R.; Ochsenfeld, C.; et al. Q-Chem 2.0: A High-Performance Ab Initio Electronic Structure Program Package. *J. Comput. Chem.* **2000**, *21*, 1532.